Colloid Polym Sci 274:654–661 (1996)

ORIGINAL CONTRIBUTION

H. Hirata
K. Maegawa
T. Kawamatsu
S. Kaneko
H. Okabayashi

Phase diagrams and phase structures of identical and mixed chain lithium di-*n*-alkyl phosphate-water binary systems. Asymmetric molecular shape effect

Received: 30 October 1995
Accepted: 5 December 1995

H. Hirata · K. Maegawa · T. Kawamatsu
S. Kaneko · Prof. H. Okabayashi (✉)
Department of Applied Chemistry
Nagoya Institute of Technology
Gokiso-cho, Showa-ku
Nagoya 466, Japan

Abstract Lithium salts of di-*n*-pentyl (DPP), *n*-butyl(*n*-hexyl) (BHP), *n*-propyl(*n*-hexyl) (PHP) and ethyl(*n*-octyl) (EOP) phosphates were synthesized and the phase diagrams of the lithium phosphate-water binary systems were determined. The phase diagrams of the DPP-, BHP- and PHP-water systems contain three regions (I, II and III) in common, which correspond to a homogeneous transparent one-phase solution, and lyotropic liquid crystalline and coagel phases, respectively. However, the EOP-H_2O system contains an additional hard gel phase (region IV).

^{31}P NMR spectra suggest that region I is a monomer ⇔ micelle equilibrium phase and region II is a lamellar phase. X-ray diffraction results show that for the DPP-, BHP- and PHP-water systems the two *n*-alkyl chains are closely packed in the lamellar phase in a manner which alternatively combines short and long chains, while in EOP-water system the two long chains are loosely packed. Furthermore, it may be assumed from ^{31}P NMR spectra and x-ray diffraction results that region IV in the EOP-water system is a cubic phase.

Thermotropic properties for these DAP-water systems were also investigated by DSC temperature profile curves. From the ΔH variation upon the II → I thermal transition, we assumed that stability of the aggregate structure in the liquid crystalline state increases in the order EOP < PHP < BHP < DPP. Thus, we have found that thermotropic properties for a series of DAP-water binary systems are closely correlated with the extent of asymmetric molecular shape in DAP.

Key words Phase diagram – identical and mixed chain di-*n*-alkyl phosphates – asymmetric molecular shape

Introduction

It is well-known that amphiphilic molecules such as surfactants, lipids, proteins and synthetic copolymers can form a variety of self-assembly structures in water. In particular, the physico–chemical properties of biological cell membranes could be successfully mimicked by using bilayer vesicles formed from naturally occurring or synthetic phospholipids. Subsequent works [1–5] have shown that simple, synthetic double-chain surfactant molecules also form vesicular assemblies with properties very similar to those of phospholipid vesicles. This made it possible to investigate the effects of structural variations in the

surfactant on the structural and functional properties of vesicle-bilayers. Thus, vesicles formed by synthetic amphiphiles offer model systems for understanding in detail the characteristic properties of biological membranes [6–16].

Israelachivili et al. [17] have shown that the type and structure of an aggregate formed by different surfactant molecules depend on their geometrical packing properties, which can be represented by the characteristic packing parameters ($v/a_0 l_c$) of a given amphiphilic molecule with optimal area a_0, hydrocarbon volume v and critical chain length l_c. In general, in a self-assembly system, the polar heads of surfactants are located at the interface between the hydrocarbon and water regions, and the relative positions and distances between the polar heads which are intimately associated with the packing state are determined mainly by their electrostatic interaction and by the packing property of the alkyl chains [17–19]. For cesium or rubidium soaps in water, it has been found that the head groups form well developed hexagonal or rectangular crystalline arrays [20]. However, they are arranged randomly, and little is known of their packing geometry. In fact, a packing property is strongly dependent on many factors, such as the ionic environment, temperature, polar-group size, and length and unsaturation of a hydrocarbon chain [21–26]. Therefore, it is very difficult to discuss quantitatively the relationship between the geometrical packing property of surfactant molecules and these many other factors. Under these circumstances it is highly desirable to undertake further systematic studies on the molecular design and synthesis of a surfactant molecule and its aggregate structure.

In order to discuss the perturbation effect of the local arrangement of polar heads on the micellar and mesomorphic properties of surfactant molecules in water, Zana et al. [27] investigated the effect of the spontaneous arrangement of the polar groups on the microstructure of the aggregates of a series of bis(quaternary ammonium bromide) surfactants, using cryogenic transmission electron microscopy. The results showed that the morphology of the aggregates depends on the molecular structures of the surfactants.

In this study, we sought to investigate the local arrangement effect of hydrocarbon moieties on the microstructures of bi-tailed surfactants. The lithium salts of di-*n*-pentyl (DPP), *n*-butyl(*n*-hexyl) (BHP), *n*-propyl(*n*-heptyl) (PHP) and ethyl(*n*-octyl) (EOP) phosphates, with characteristic packing parameters equal to 0.50, 0.43, 0.37 and 0.33, respectively, were synthesized, and the phase diagrams and phase structures of these double chain surfactant-water systems were determined. In particular, by using the thermotropic data of these phosphate-water binary systems, we discuss the stability of the liquid crystalline structure formed by these phosphate anions in terms of their asymmetric molecular shape.

Experimental

Materials

Lithium salts of di-*n*-pentyl (DPP), *n*-butyl(*n*-hexyl) (BHP), *n*-propyl(*n*-heptyl) (PHP) and ethyl(*n*-octyl) (EOP) phosphates were prepared as follows. *n*-Alkyl phosphorodichloridates ($R–OP(O)Cl_2$) prepared using phosphoryl chloride and the corresponding alcohol (ROH, R: shorter chain) and vacuum-distilled several times. The $R–OP(O)Cl_2$ samples were converted to identical- and mixed-chain di-*n*-alkyl phosphorochloridates, (R–O)(R′–O)P(O)Cl, by treated with corresponding alcohol (R′OH, R′: longer chain) [28], and vacuum-distilled several times. The boiling points of $R–OP(O)Cl_2$ and (R–O)(R′–O)P(O)Cl are listed in Table 1. (R–O)(R′–O)P(O)Cl were treated with benzaldoxim (Furuka Chemie AG) by the method of Mukaiyama et al. [29], to yield phosphoric acid di-*n*-alkylesters, (RO)(R′O)P(O)OH. Phosphoric acid di-*n*-alkyl esters were finally neutralized with lithium hydroxide aqueous solution, and the lithium salts were recrystallized in aqueous acetone. The series of di-*n*-alkyl phosphate lithium salts thus obtained are termed DAP. The sample identity was confirmed by ^1H and ^{13}C NMR and by elemental analyses. The agreement between the calculated and observed values of elemental analyses were within 0.2% (Scheme 1).

Phase diagram determinations and calorimetry

Sample solutions were prepared by weighing the DAP and water components into glass ampoules, which were then sealed and the contents homogenized by heating and shaking. The temperature dependence of the phase feature of the samples was determined by visual inspection as the ampoules were held in a temperature-controlled water-bath (rate of temperature elevation and cooling

Table 1 The boiling points of $R–OP(O)Cl_2$ and (R–O)(R′–O)P(O)Cl

	$R–OP(O)Cl_2$	(R–O)(R′–O)P(O)Cl
DPP	75 ~ 77 °C at 4 mmHG	108 ~ 110 °C at 4 mmHg
BHP	73 ~ 75 °C at 4 mmHg	110 ~ 113 °C at 4 mmHg
PHP	59 ~ 61 °C at 4 mmHg	111 ~ 113 °C at 4 mmHg
EOP	65 ~ 68 °C at 25 mmHg	117 ~ 119 °C at 4 mmHg

Colloid & Polymer Science, Vol. 274, No. 7 (1996)

Scheme 1

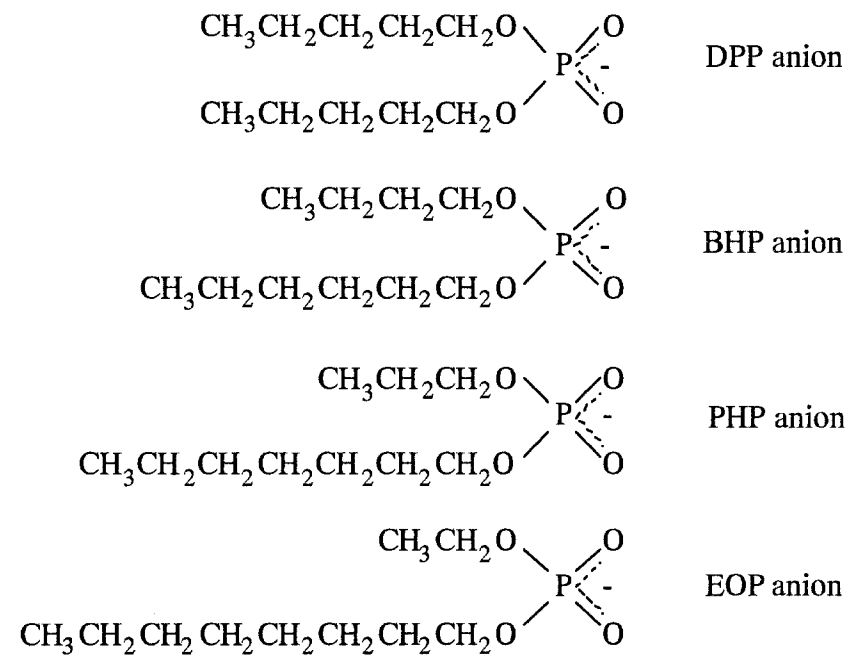

0.1 °C/min). The temperature was measured with a digital thermometer (Sato Keiryoki).

The thermotropic transition temperatures of the DAP-water systems were determined with a differential scanning calorimeter (Rigaku DSC 8230), which was scanned at a rate of 2 °C/min by using a volatile pan with α-Al_2O_3 in the reference pan.

^{31}P and ^{2}H NMR and x-ray diffraction measurements

^{31}P NMR spectra were measured using high-power proton decoupling at 80.995 MHz on a Varian XL-200 spectrometer. The ^{31}P chemical shifts (σ) of the DAP anions in D_2O solution were measured relative to the ^{31}P signal of aqueous 85%-H_3PO_4 solution as an external reference.

^{2}H NMR spectra were measured on a Varian XL-200 NMR spectrometer (30.71 MHz) with a spectral width of 15000 Hz, 16384 points in the time domain and an acquisition time of 0.5 ~ 2 s. All the ^{2}H NMR measurements were made after thermal equilibrium of the samples had been confirmed.

The x-ray diffraction low-angle patterns were obtained using a RU-200 camera (Rigaku Denki Co.) with a three slit-system in the diffraction range of $1.2° < 2\theta < 10°$. Nickel-filtered CuKα radiation (λ = 1.54 Å) was used. The temperature of the sample was controlled by air within $\pm$ 1°C and was measured with a digital thermometer (Sato Keiryoki).

Results and discussion

Phase diagrams of the DAP-H_2O systems and phase structure

Figure 1 shows the phase diagrams of the DAP-H_2O systems. For the DPP-, BHP- and PHP-H_2O binary systems, the phase diagrams consist of three regions (I, II and III). For region I, a homogeneous and transparent isotropic solution was obtained in common for the three systems. In region II, a lyotropic liquid crystalline state was obtained. The optically-isotropic property of region I and the lyotropic liquid crystalline state of region II were confirmed under a polarizing microscope. Region III was a coagel phase.

For the EOP-H_2O system, the phase diagram consists of four regions (I, II, III and IV) [30]. The regions I, II and III are an isotropic solution, and lyotropic liquid crystalline and coagel phases, respectively. In region IV, a homogeneous and transparent hard gel phase was obtained.

For the DAP sample solutions in region I, only narrow and symmetrical ^{31}P NMR signals were observed in common. The ^{31}P chemical shifts (σ), which are sensitive to the formation of aggregates [31–34], were measured at various concentrations. The result shows that there exists a critical micelle concentration (CMC) in region I, indicating the presence of a monomer $\Leftrightarrow$ micelle equilibrium. The CMCs are 5.0 wt% for DPP, 4.3 wt% for BHP, 3.7 wt% for PHP and 2.3 wt% for EOP.

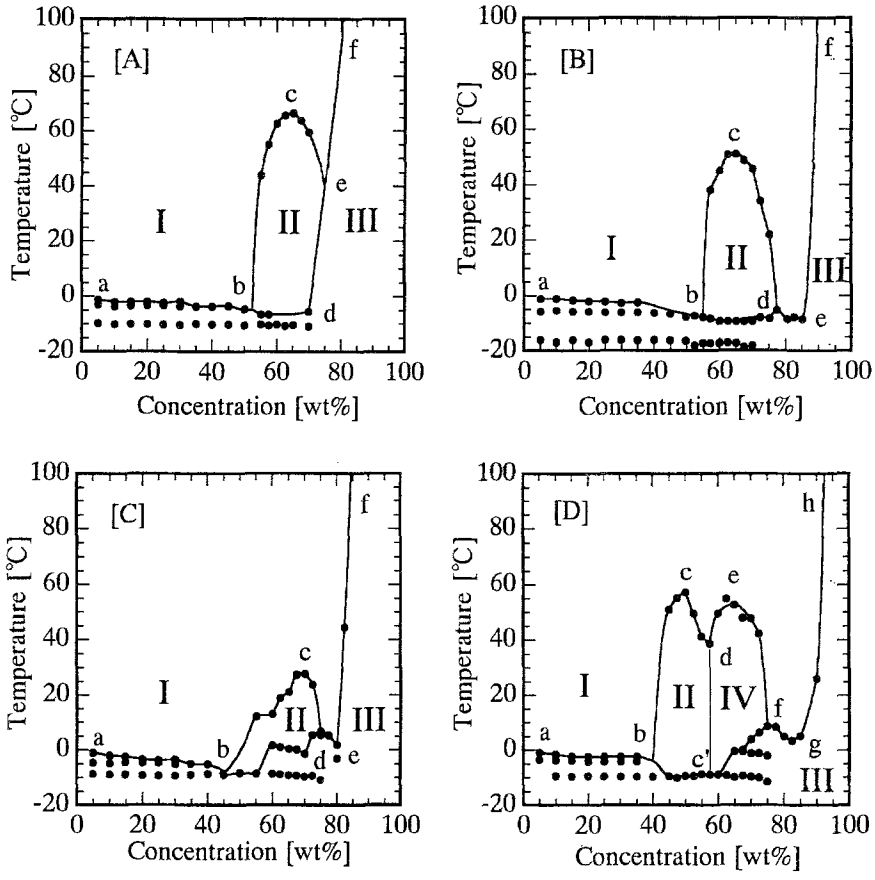

Fig. 1 Phase diagrams of the DAP-water binary systems ([A], DPP-H_2O; [B], BHP-H_2O; [C], PHP-H_2O; [D], EOP-H_2O). The solid lines show the phase boundary assumed by visual inspection and the filled circles denote the phase transition temperatures obtained from the DSC temperature elevation curves. Region I: homogeneous aqueous solution; region II: lyotropic liquid crystalline phase; region III: coagel phase for the DPP-, BHP-, PHP-H_2O systems, (below the line **abdef**) and for the EOP-H_2O system (below the line **abc'fgh**), region IV: hard gel phase

As shown in Fig. 2, low-field shoulders were found in the ^{31}P NMR spectra of the DAP samples in region II and the spectral features are similar to that of the bilayer-type sodium dibutyl phosphate [35]. Such characteristic asymmetry is due to the chemical shift anisotropy ($\Delta\sigma$) of a ^{31}P nucleus in the polar group, arising from the restricted anisotropic motion of the DAP anions [36]. It can be seen that the $\Delta\sigma$ value becomes small in the order EOP < PHP < BHP < DPP, showing that the asymmetric molecular shape of these dialkyl phosphates affects the ^{31}P chemical shifts anisotropy of a ^{31}P nucleus. In order to discuss the differences in $\Delta\sigma$ of these compounds in detail, the molecular conformational study of these dialkyl phosphates by x-ray crystallographic methods, and theoretical calculations of the chemical shift shielding tensors of dialkyl phosphate are highly desirable. Anyway, we may assume that region II is more structurally organized compared with region I and that a lamellar-like structure exists in this region.

The x-ray low-angle diffraction patterns of the DAP samples in region II were measured at various concentrations. Wide and diffuse reflections were observed. It was found that the interplaner spacing (d) strongly depends on both the DAP content and the species of DAP and a increase in DAP content results in a decrease in the d value (Fig. 3). Moreover, the d value was found to increase in the order of DPP < BHP < PHP < EOP. In particular, the increase in d were most clearly seen between PHP and EOP. Since the radial electron density distributions calculated by Fourier transformation of the x-ray diffraction intensities become a measure of the distance between two polar layers sandwiched by hydrocarbon layers, the observed d values provide information on the structure of the bilayer-type aggregates [37]. Therefore, this observation indicates that the thickness of the bilayer in a lamellar-type structure and d increase in the same order. The differences in d during DPP, BHP and PHP are not so marked. However, there exists a marked difference in d between PHP and EOP. The results may be explained as follows.

In the case of DPP the structural model similar to the bilayer formed by lipid molecules can be presented (Fig. 4). When mixed chain di-*n*-alkyl phosphates make up the bilayer-type structure, we may assume that the two di-*n*-alkyl chains are closely packed in a manner which alternatively combines short and long *n*-alkyl chains (Fig. 4 [A]).

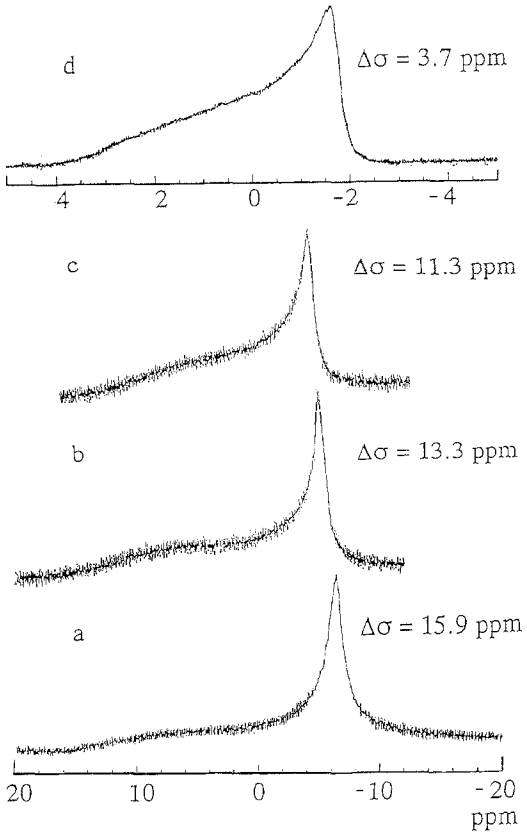

Fig. 2 ^{31}P NMR spectra of the samples in region II at 25 °C (a: DPP 70 wt%, b: BHP 70 wt%, c: PHP 70 wt% and d: EOP 50 wt%) and the chemical shift anisotropies ($\Delta\sigma$)

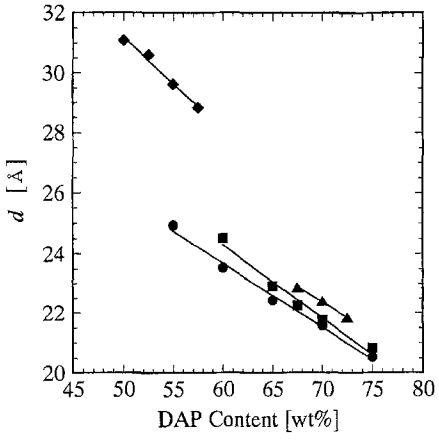

Fig. 3 Concentration dependence of the d values for the DAP-water systems (DPP (●); BHP (■); PHP (▲); EOP (◆)) at 25 °C

In such a closely packed bilayer, the thickness of the bilayer formed by mixed chain dialkyl phosphates should be equal to that for DPP. The observed data are not in accord with the results assumed by the model. Probably,

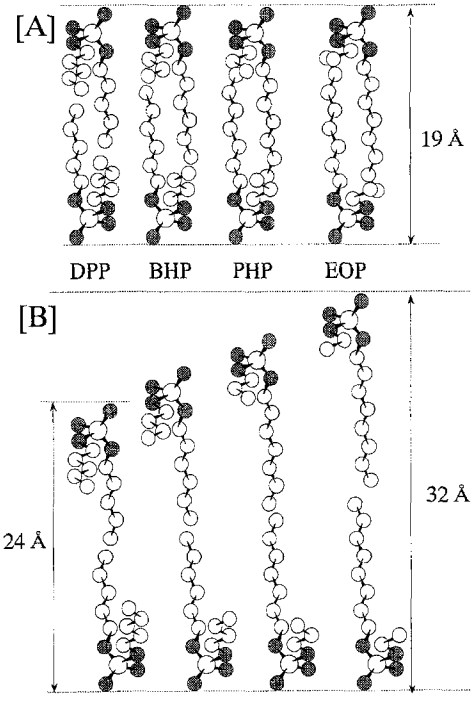

Fig. 4 Schematic model of DPP bilayers. [A] : closely packed structure, [B] : loosely packed structure

this disagreement comes from the differences in segmental mobility for shorter n-alkyl chains. In general, it has been found for surfactant molecules in aqueous solutions that as the length of n-alkyl chain decreases the segmental mobility progressively increases. This is also the case for DAP in aqueous solutions. Therefore, we may assume that the segmental mobility of shorter n-alkyl chains increases in the order BHP < PHP < EOP, preventing the formation of a closely packed structure. Thus, the contribution of a loosely packed structure to the thickness of a bilayer increases, resulting in the progressive increase in thickness. For EOP, in particular, a loosely packed model (Fig. 4 [B]) rather than a closely packed model may be applied, since the orientation of ethyl group at the interface of a bilayer may be disturbed owing to the small hydrophobicity and high segmented mobility.

For the EOP-H_2O binary system, region IV is a hard gel phase. The samples in region IV provide a very sharp ^{31}P NMR signal which corresponds well to that of cubic phase [38]. The x-ray low-angle diffraction patterns of EOP samples in region IV were also measured at various concentrations. The SAXS data from the cubic phase revealed two strong peaks. The corresponding lattice parameters for the two samples were found to be 28.30 and 24.66 Å for 60 wt% and 27.08 and 23.48 Å for 65 wt%. Although the number of reflections is not sufficient for an

unambiguous indexing, we have found that the data fit reasonably well to a face-centered-cubic structure [39].

Thermotropic properties of the DAP-H_2O systems

Figure 5 shows DSC curves for the DAP-H_2O solutions and describes the variation of the phase transition with water content. The phase transition temperatures for representative samples are listed in Table 2 together with the ΔH values calculated from the peak area. For these DSC curves, endothermic peaks were found in the temperature range $-20 \sim 10\,^{\circ}C$. In order to investigate the nature of the thermal transitions, DSC measurements were also made for the DAP-D_2O systems. The corresponding endothermic peaks shifted to a higher temperature by $4\,^{\circ}C$ with respect to those of the DAP-H_2O systems. If one considers that the melting point of pure D_2O is about $4\,^{\circ}C$ higher than that of pure H_2O [40], the result suggests that the thermal transitions are ascribed to melting of bulk-like water in the aggregates formed by DAP anions. Thus, for the DAP sample solutions (10 wt%), the thermal transitions starting at $-2.1\,^{\circ}C$ (DPP), $-1.3\,^{\circ}C$ (BHP), $-1.9\,^{\circ}C$ (PHP) and $-1.6\,^{\circ}C$ (EOP) are ascribed to melting of bulk-like water.

The endothermic peak 1 which corresponds to the melting of bulk-like water in DAP samples disappeared at the concentration of 45 wt%, indicating that above 45 wt% all the water molecules may be allowed to exist as a kind of bound water which is incorporated between

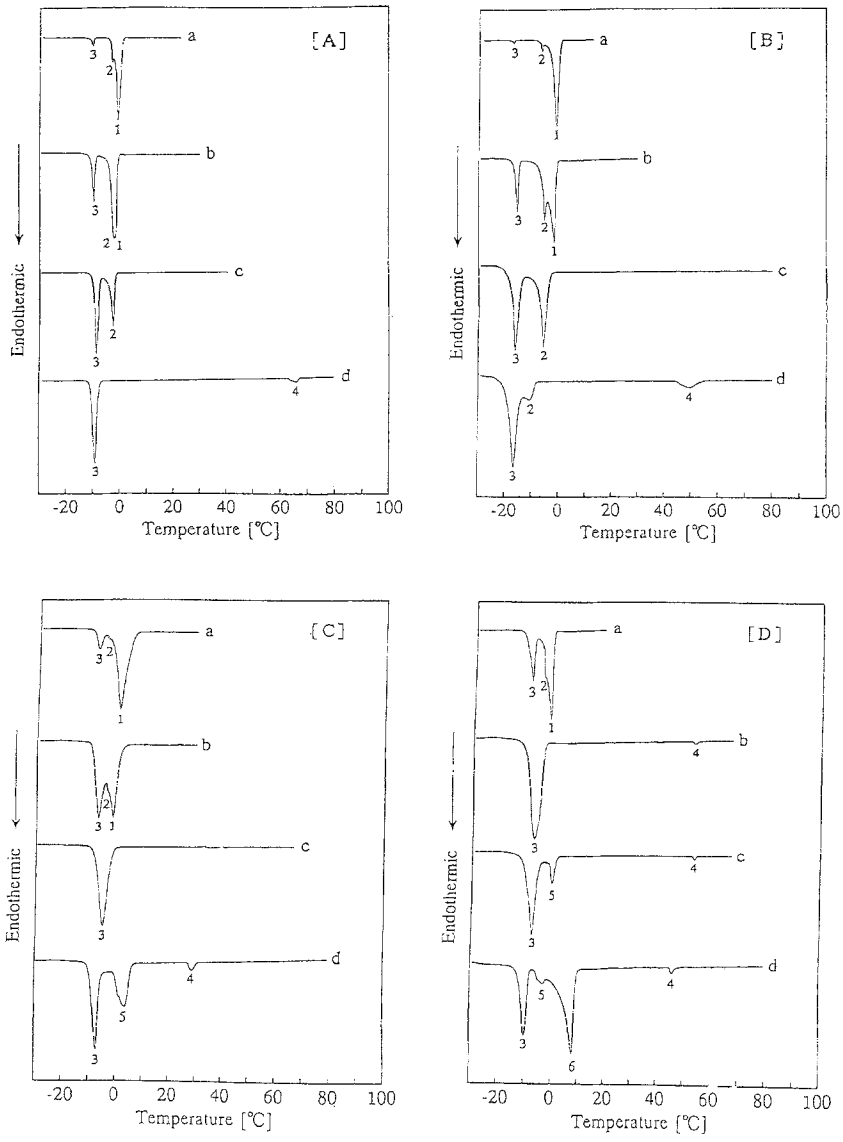

Fig. 5 Representative DSC curves of the DAP-water systems.
[A] : DPP-H_2O (a: 10 wt%, b: 30 wt%, c: 50 wt% and d: 70 wt%); [B] : BHP-H_2O (a: 10 wt%, b: 30 wt%, c: 50 wt% and d: 70 wt%); [C] : PHP-H_2O (a: 10 wt%, b: 30 wt%, c: 50 wt% and d: 70 wt%); [D] : EOP-H_2O (a: 30 wt%, b: 50 wt%, c: 60 wt% and d: 70 wt%)

Colloid & Polymer Science, Vol. 274, No. 7 (1996)

Table 2 Phase transition temperature (T_t, °C) and ΔH ($J\,g^{-1}$ of sample) for the DAP-water systems

Sample	C [wt%]	Peak 3		Peak 2		Peak 1		Peak 6		Peak 5		Peak 4	
		T_t	ΔH	T_t	ΔH	T_t	ΔH	T_t	ΔH	T_t	ΔH	T_t	ΔH
DPP	10	−10.1	15.4	−3.6	24.6	−2.1	240.8	*	*	*	*	*	*
	30	−10.3	52.4	−3.5	*	2.0	*	*	*	*	*	*	*
	50	−10.4	96.7	−4.7	*	*	*	*	*	*	*	*	*
	60	−10.2	123.4	*	*	*	*	*	*	*	*	62.7	9.5
	70	−10.8	*	*	*	*	*	*	*	−5.5	*	59.5	10.8
BHP	10	−16.8	9.1	−5.5	38.5	−1.3	243.5	*	*	*	*	*	*
	30	−16.1	42.2	−6.1	*	−2.7	*	*	*	*	*	*	*
	50	−16.3	60.2	−7.6	*	*	*	*	*	*	*	*	*
	60	−17.2	*	*	*	*	*	*	*	−9.3	*	45.2	7.2
	70	−18.5	*	*	*	*	*	*	*	−9.3	*	45.8	9.3
PHP	10	−8.8	40.0	−4.6	40.4	−1.9	242.5	*	*	*	*	*	*
	30	−9.2	125.6	−5.1	*	−3.4	*	*	*	*	*	*	*
	50	−8.3	*	*	*	*	*	*	*	*	*	*	*
	60	−8.5	*	*	*	*	*	*	*	1.7	*	13.1	2.7
	70	−9.7	*	*	*	*	*	*	*	−1.3	*	27.9	6.3
EOP	10	−9.5	38.2	−3.6	65.7	−1.6	241.2	*	*	*	*	*	*
	30	−9.7	116.5	−4.2	*	−2.3	*	*	*	*	*	*	*
	50	−9.3	101.6	*	*	*	*	*	*	*	*	57.2	1.5
	60	−8.8	*	*	*	*	*	*	*	*	*	49.6	2.5
	70	−9.6	*	*	*	*	*	−1.1	*	3.9	*	47.6	2.0

bilayers of lamellar structures and does not crystallize on cooling down to −30 °C [40].

In order to investigate the cause of peaks 2 and 3, the temperature dependence of the ^{2}H-NMR spectrum for the DAP-D_2O systems was measured. The results are briefly described below [41].

It was found that the spectral features of the ^{2}H-NMR and ^{31}P-NMR strongly depend on temperature. Below the transition temperature of peak 3, only symmetrical and broad ^{2}H and ^{31}P resonance signals were observed, while, above that of peak 3, ^{2}H-NMR powder patterns [35, 42] and ^{31}P-NMR spectral patterns characteristic of a lamellar structure [35–37] were observed. This observation indicates that the peak 3 derives from the disorder to lamellar transitions. Above the transition temperature of peak 2, only symmetrical and sharp ^{2}H and ^{31}P resonance were observed, showing that the peak 2 comes from the lamellar to disorder transition.

For the concentrated samples, it was found that the areas of two endothermic peaks deriving from peak 1 and peak 2 tend to become very small or disappear as the peak 3 becomes predominant. Furthermore, we found that the thermal transition peaks 5 and 6 for the DSC curve of the concentrated PHP sample (70 wt%) and for that of the EOP samples (70 wt%) appear. The endothermic peaks 5 for PHP and EOP should be due to the coagel to liquid crystal transition. For concentrated samples of the DPP- and BHP-water systems, similar observations were made.

Recently, we have reported that the conformational preference about the P-O bonds depends upon the extent of hydration and occurs for both identical and mixed chain di-*n*-alkyl phosphate sodium salt-water systems in the coagel state [43, 44]. This fact implies that the aggregate structure of these systems in the coagels depends upon the hydrated environment of the phosphate group. Thus, for the coagel samples of PHP and EOP, we may also assume that the conformational preference about the P-O bond occurs at the transition temperatures. The endothermic peaks 6 may be related to the conformational preference about the P-O bonds. Further investigation is highly desirable, in order to elucidate the cause of this transition. For the DAP samples in the lyotropic liquid crystalline state, endothermic peaks (peak 4) are observed in common in the temperature range 40 ~ 80 °C (Fig. 5), and may be caused by variation of the molecular ordering of the aggregates upon the lyotropic to the isotropic transition (II → I transition), since none of these peaks shifted to a higher temperature when D_2O was used as solvent. Figure 6 shows the concentration dependence of the ΔH value for the endothermic peaks derived from the II → I thermal transition. The ΔH values tend to increase with an increase in concentration, showing that the aggregate structure of DAP anions in the liquid crystalline state is stabilized with increasing concentration. Furthermore, it should be emphasized that the extent of variation in the ΔH value depends upon the species of DAP. That is, the extent of ΔH variation increases in the order EOP < PHP <

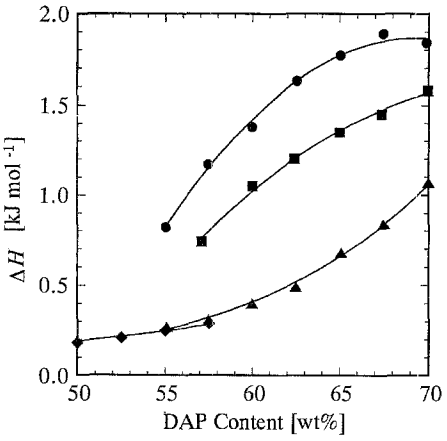

Fig. 6 Concentration dependence of the ΔH value due to the II → I transition in the DAP-water systems (DPP (●); BHP (■); PHP (▲); EOP (♦))

BHP < DPP, suggesting that the stability of the aggregate structure in the liquid crystalline state also increases in this order.

For the DSC curves of the EOP-H_2O samples in region IV, in which the samples are in a hard gel state, the endothermic peaks (peak 4) are also observed in the temperature range 45° ~ 50 °C, and may be ascribed to variation in the structural ordering of the aggregates upon the hard gel to the isotropic transition, since none of these peaks shifted to a higher temperature when D_2O was used as solvent.

Acknowledgment We express gratitude to Prof. Charmian J. O'Conner (University of Auckland, Department of Chemistry, New Zealand) and Dr. Gerd Olofsson (University of Lund, Division of Thermochemistry, Chemical Center, Sweden) for reading the manuscript prior to publication and making suggestions for its revision.

References

1. Kunitake T, Okahata Y (1977) J Amer Chem Soc 99:3860–3862
2. Fendler JH (1980) Acc Chem Res 13:7–13
3. Fuhrhop JH, Mathieu J (1984) Angew Chem 96:124–137
4. Sudhölter EJR, Engberts JBFN, Hoekstra D (1980) J Amer Chem Soc 102:2467–2469
5. Sudhölter EJR, De Grip WJ, Engberts JBFN (1982) J Amer Chem Soc 104:1069–1072
6. Kano K, Romero A, Djermouni B, Acke HJ, Fendler JH (1979) J Amer Chem Soc 101:4030–4037
7. Kumano A, Kajiyama T, Takayanagi M, Kunitake T, Okahata Y (1984) Ber Bunsen-Ges Phys Chem 88:1216–1222
8. Shimomura M, Kunitake T (1982) J Amer Chem Soc 104:1757–1759
9. Murakami Y, Nakano A, Yoshimatsu A, Uchitomi K, Matsuda Y (1984) J Amer Chem Soc 106:3613–3623
10. Carmona-Ribeiro AM, Chaimovich H (1983) Biochim Biophys Acta 733:172–179
11. Carmona-Ribeiro AM, Yoshida LS, Sesso A, Chaimovich H (1984) J Colloid Interface Sci 100:433–443
12. Rupert LAM, Hoekstra D, Engberts JBFN (1985) J Amer Chem Soc 107:2628–2631
13. Rupert LAM, Engberts JBFN, Hoekstra D (1986) J Amer Chem Soc 108:3920–2925
14. Rupert LAM, Van Breemen JFC, Van Bruggen EFJ, Engberts JBFN, Hoekstra D (1987) J Membr Biol 95:255–263
15. Rupert LA, Hoekstra D, Engberts JBFN (1987) J Colloid Interface Sci 120: 125–134
16. Shimomura M, Kunitake T (1981) Chem Lett 1001–1004
17. Israelachvili JN, Mitchell DJ, Ninham BW (1976) J Chem Soc Faraday Trans I 72:1525–1568
18. Ekwall P (1975) Adv Liq Cryst 1:1–142
19. Skoulios A (1979) Am Phys 3:421–450
20. Vincent JM, Skoulios A (1966) Acta cryst 20:432–440, 441–446, 447–451
21. Puvvada S, Blanckstein D (1990) J Chem Phys 92:3710–3724
22. Kato T, Seimiya T (1986) J Phys Chem 90:3159–3167
23. Herrington TM, Sahi SS (1988) J Colloid Interface Sci 121:107–120
24. Missel PJ, Mazer NA, Benedek GB, Young CY, Carey MC (1980) J Phys Chem 84:1044–1057
25. Malliaris A, Le Moigne J, Sturm J, Zana R (1985) J Phys Chem 89:2709–2713
26. Carnie SL, Israelachvili JN, Pailthorpe BA (1979) Biochim Biophys Acta 554: 340–357
27. Zana R, Talmon Y (1993) Nature 362: 228–230
28. McCombie H, Saunders BC, Stacey GJ (1945) J Chem Soc 380–382
29. Mukaiyama T, Fujisawa T (1961) Bull Chem Soc Jpn 34:812–813
30. Hirata H, Katayama S, Okabayashi H, Furusaka M, Kawakatsu T (1995) Colloid Polym Sci in press
31. Roberts MF, Adamich M, Robson RJ, Dennis EA (1979) Biochemistry 18: 3301–3308
32. Matsushita K, Kamo O, Terada Y, Yoshida T, Okabayashi H (1984) Chem Scripta 23:228–232
33. Crutchfield MM, Callis CF, Irani RR, Roth GC (1962) Inorg Chem 1:813–817
34. Jardetsky O, Wertz JE (1960) J Amer Chem Soc 82:318–323
35. Chachaty C, Quagebeur JP (1983) J Phys Chem 87:4341–4343
36. Yoshida T, Miyagai K, Taga K, Okabayashi H, Matsushita K (1990) Magn Reson Chem 28:715–721
37. Yoshida T, Miyagai K, Aoki S, Taga K, Okabayashi H (1991) Colloid Polym Sci 269:713–719
38. Cullis PR, de Kruijff B (1979) Biochem Biophys Acta 559:399–420
39. Lawaon KD, Mabis AJ, Flautt TJ (1968) J Phys Chem 72:2058–2065
40. Kodama M, Kuwabara M, Seki S (1982) Biochem Biophys Acta 689:567–570
41. Hirata H, Ogasawara T, Okabayashi H, unpublished data to be published separately
42. Ulmius J, Wennerstrom H, Lindblom G, Arvidson G (1977) Biochemistry 16: 5742–5745
43. Okabayashi H, Taga K, Miyagai M, Uehara T, Yoshida T, Nishio E (1991) J Phys Chem 95:7932–7938
44. Okabayashi H, Hirata H, Suzuki Y, Taga K, Mathew C (1995) Vibrational Spectroscopy in press